The Institute of Space and Astronautical Science
Report No. 655, December 1994

Wind Tunnel Experiments on Wake Flow Field behind a Reentry Capsule from a Viewpoint of Parachute Deployment at Supersonic Speeds

By

Kojiro SUZUKI and Takashi ABE

(August 25, 1994)

ABSTRACT: The wake flow field behind the EXPRESS capsule at supersonic speeds is studied experimentally in the wind tunnel. The schlieren photographs and the measurements of the Pitot pressure and the static pressure in the wake clarify the structure of the wake flow field and the effects of the freestream Mach number on it. The wake structure is classified into two types, that is, the subsonic wake neck type and the supersonic wake neck type. The flow characteristics of each wake neck type are discussed. From a viewpoint of the parachute deployment, the effects of the freestream Mach number on the dynamic pressure in the wake are investigated. The recovery ratio of the dynamic pressure in the wake increases with the decrease in the Mach number. At lower Mach number, however, the recovery is delayed due to the extension of the recirculating region behind the capsule bottom. The numerical simulations of the wake flow field are carried out by solving the laminar Navier-Stokes equations and it is pointed out that the recovery of the flow velocity and the dynamic pressure may be enhanced significantly by the turbulent transition on the wake trail.

NOMENCLATURES

D	Base diameter
M	Local Mach number
p	Local static pressure
p_0	Local total pressure
p_{pitot}	Local Pitot pressure
q	Local dynamic pressure
Re_D	Freestream Reynolds number based on D $(=\rho_\infty U_\infty D/\mu_\infty)$
U_∞	Freestream velocity
x	Distance measured from body base along body axis
y	Normal distance measured from body axis
γ	Ratio of specific heat (taken as 1.4 for air)
ρ_∞	Freestream density
μ_∞	Viscosity of freestream air
Subscript	
∞	Freestream value

1. INTRODUCTION

When a reentry vehicle of capsule type is used for the recovery of a payload from an earth orbit, the parachute is often used at supersonic speeds in order to enhance the deceleration and the stability of the vehicle in advance to the deployment of the main parachute at landing. In the transonic regime, it is known that the static stability on the pitching plane is significantly reduced for the blunted-cone type vehicle. In order to avoid undesirable spin motions from a viewpoint of the safety in the recovery of the payload, the parachute should be deployed at supersonic speed before the flight Mach number reaches the transonic regime. In fact, in a series of the wind tunnel experiments made for the "EXPRESS" capsule [*1*] configuration, it is pointed out that the static stability vanishes at Mach number 1.3 when the center of gravity is assumed to be located at the center of the capsule. In this case, the parachute deployment must be completed by this Mach number.

The efficiency of the deceleration of the vehicle by the parachute strongly depends on the aerodynamic properties (especially on the dynamic pressure) in the wake flow field behind the body. In general, when the dynamic pressure is high at the place where the parachute is deployed, the drag force generated by the parachute is also large and, as a result, a large deceleration force is produced for the vehicle. In the wake flow field behind a bluff body such as the "EXPRESS" capsule flying at a supersonic speed, the dynamic pressure is much lower than the freestream dynamic pressure and the ratio of the local dynamic pressure to its freestream value significantly varies both with the freestream Mach number and with the distance from the bottom of the capsule. Then the deceleration force produced by the parachute depends both on the flight Mach number and on the distance between the capsule bottom and the parachute canopy.

At the deployment of the parachute, the vehicle may experience two kinds of strong shock forces named as the snatch force and the opening force [*2*]. The former is produced by the release of the parachute from the capsule and the latter is by the deployment of the parachute. In case of the parachute deployment at supersonic speeds, the former is known to be much greater than the latter. Considering the damage to the payload accommodated inside the capsule, it is required to make these shock forces as small as possible. The snatch force is reduced by shortening the distance between the capsule body and the parachute [*2*]. On the other hand, from a viewpoint of the decelerating force produced by the parachute, the parachute should be deployed as far as possible from the capsule, since the dynamic pressure in the wake region increases with the increase in the distance from the capsule bottom. It is necessary to find the optimum place both for the snatch force and for the decelerating force. Then it is strongly demanded for the design of the parachute system to predict the aerodynamic properties in the wake flow field behind the capsule, especially the dynamic pressure in the wake region.

In order to predict the distribution of the dynamic pressure in the wake region, the structure of the wake flow field should be clarified. Figure 1 (adopted from Ref. 3) explains the schematic view of the wake structure behind a supersonic blunted body with a flat bottom. First, the bow shock wave is formed over the body and separates the whole flow field into the freestrream region and the region disturbed by the presence of the body. In the vicinity of the body, there is a boundary layer that will separate at the corner of the base and develop as a "shear-layer" behind the capsule bottom. The recirculating region which is bounded by the shear-layer will shrink in the downstream direction and form the "wake-neck". In the neighborhood of the wake neck, a recompression of the flow is attained through the "trailing shock". The recirculating region ends at the "rear stagnation point", where the flow velocity vanishes. It should be noted that the wake neck is not necessarily located in the downstream of the rear stagnation point as illustrated in Fig. 1. In the downstream region from the wake neck, the "wake core" is formed around the center line of the wake. The wake core will diffuse when the flow goes downstream. The dynamic pressure is at the minimum in the recirculating region and the recovery of the dynamic pressure begins behind the recirculating region.

The present experimental investigations are focused mainly on the flow properties in the downstream region of the wake neck, since the parachute will be deployed at the distance larger than five-times of the base diameter from the capsule bottom.

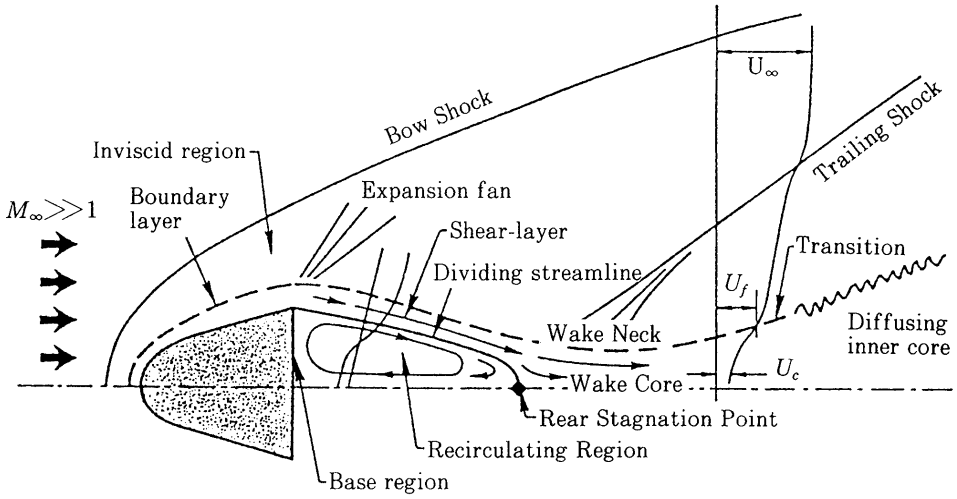

Fig. 1. Schematic View of Wake Structure behind Supersonic Body with Flat Base (from Ref. 3).

The problem of the wake flow field is also important from a viewpoint of the aerothermodynamic environment on the vehicle bottom at the hypersonic flight. As for the aerodynamic heating to the base surface, the convective heating depends on the transport properties in the recirculating region and the radiative heating is strongly affected by the presence of the high temperature zone due to the recompression of the flow at the wake neck. In past experiments, significant gas luminosity in the wake neck region was observed [*4*]. If the effects of the Mach number on the geometry of the wake structure including the location of the wake neck are clarified by the supersonic wind tunnel experiments, it will be of help in the prediction of the aerothermodynamic environment in the base region of the space vehicle flying at hypersonic speeds.

In the present study, experimental investigations on the wake flow field behind the "EXPRESS" reentry vehicle are carried out at Mach numbers from 1.3 to 4.2 by using the transonic and supersonic wind tunnels. Considering that the parachute deployment should be completed by the time when the static stability of the vehicle pitch motion disappears in the transonic regime, the lowest experimental Mach number is set to be 1.3. The experimental Mach number is varied up to 4.2 in order to investigate the effects of the Mach number on the properties and the structure of the wake flow field. The flow visualization by the schlieren method is made to clarify the structure of the wake flow field. The measurements by traversing the Pitot pressure probes and the static pressure probe will provide both qualitative and quantitative informations on the wake flow field, especially the recovery of the dynamic pressure in the downstream region of the wake neck. The angle of attack is fixed as 0-deg in the present study, since the "EXPRESS " vehicle is a reentry vehicle of non-lifting type flying at the angle of attack around 0-deg. To deepen our understanding on the structure of the wake flow field, the numerical simulations by solving the laminar axi-symmetric Navier-Stokes equations are also carried out. We discuss qualitatively and quantitatively the validity of the results of the Navier-Stokes analysis by the comparisons with the experimental results.

The major objectives in the present study are as follows:

(1) To clarify the structure of the wake flow field by the schlieren flow visualization and to investigate the mechanism of the recovery of the flow properties in the wake by comparing the

Pitot pressure distribution with the schlieren picture,
(2) To clarify the effects of the freestream Mach number on the structure of the wake flow field,
(3) To obtain the spatial distribution of the dynamic pressure in the wake region behind the "EXPRESS" reentry capsule at various supersonic Mach numbers by the wind tunnel experiments,
(4) To clarify the effects of the freestream Mach number on the recovery of the dynamic pressure in the wake flow field,
(5) To make the validation of the Navier-Stokes analysis qualitatively and quantitatively by the comparisons with the experimental results.

2. EXPERIMENTAL MODELS AND APPARATUS

Test Facilities

The present experiments have been carried out in two series of tests. One is the Mach number sweep test to investigate the effects of the Mach number on the wake flow field and the other is the Reynolds number sweep test to investigate the effects of the Reynolds number. All the experiments have been conducted at the ISAS, Sagamihara campus, 60 × 60-cm transonic and supersonic wind tunnels. The test Mach numbers and the characteristic flow properties are summarized in Table 1:

Table 1. Test Conditions

Mach Number Sweep

Wind Tunnel Test Facility	M_∞	p_0 (Ejector) (kgf/cm^2)	p_∞ (kgf/cm^2)	q (kgf/cm^2)	Re_D ($\times 10^6$)
60 × 60-cm Transonic	1.3	1.5	0.56	0.64	1.8
60 × 60-cm Supersonic	1.6	1.8 (OFF)	0.41	0.76	2.1
	2.0	2.2 (OFF)	0.27	0.78	2.2
	3.0	4.5 (OFF)	0.12	0.75	2.7
	4.2	5.3 (ON)	0.03	0.33	1.9

Reynolds Number Sweep

Wind Tunnel Test Facility	M_∞	p_0 (Ejector) (kgf/cm^2)	p_∞ (kgf/cm^2)	q (kgf/cm^2)	Re_D ($\times 10^6$)
60 × 60-cm Supersonic	3.1	2.3 (ON)	0.06	0.37	1.4
	3.0	4.5 (OFF)	0.12	0.75	2.7
	3.0	6.5 (OFF)	0.17	1.10	4.2

In the supersonic tunnel, the settling chamber pressure, in other words, the stagnation pressure, is reduced by use of the ejector installed in the downstream of the test section. The Reynolds number sweep test is carried out at Mach number 3 by varying the settling chamber pressure with the assist of the ejector. Figure 2 shows the variations of the freestream Reynolds number referred to the base diameter with the Mach number. The freestream Reynolds number varies slightly with the Mach number even in the Mach number sweep test.

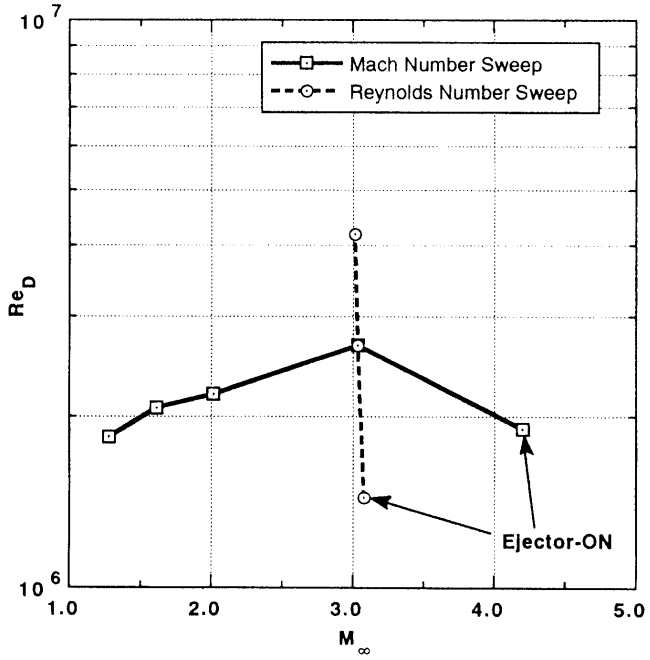

Fig. 2. Variation of Freestream Reynolds Number with Mach Number in Wind Tunnel Experiments.

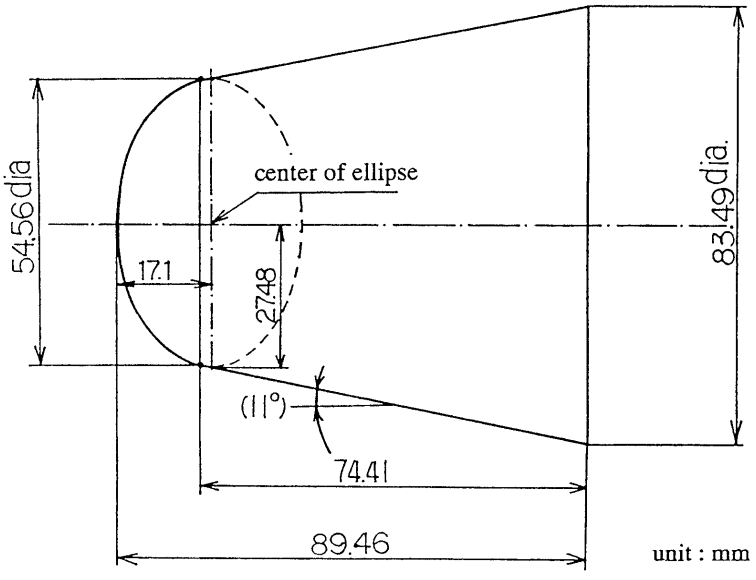

Fig. 3. Exeprimental Model of EXPRESS Reentry Capsule.

Test Model and Measuring System

The 6% scale model of the "EXPRESS" reentry capsule is used for the present study. The capsule configuration is an ellipsoidally blunted cone with 11-degree cone-half angle as shown in Fig. 3. The model is made of stainless steel. Figure 4 shows the setups of the model in the transonic and supersonic wind tunnels. Both the transonic wind tunnel and the supersonic wind tunnel have test sections of 60 × 60-cm square and the blockage ratio for the present model is about 1.5%, which is below the operation limit for both of the wind tunnels. In order to reduce the aerodynamic disturbances of the model support to the wake flow field, the model is supported on the conical

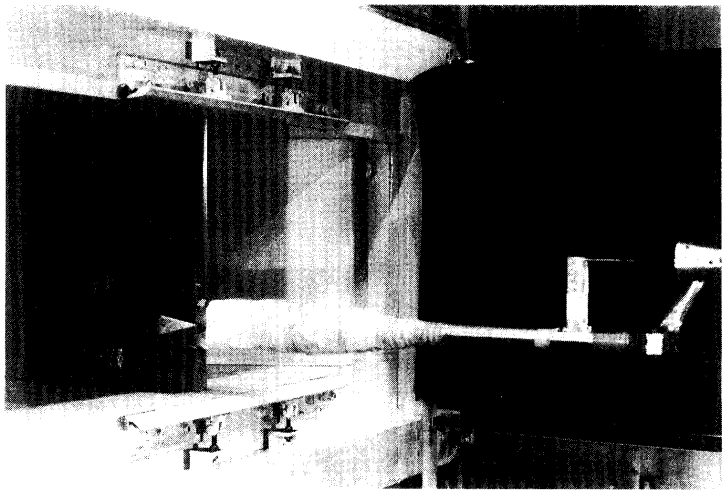

MODEL SETUP IN TRANSONIC WIND TUNNEL

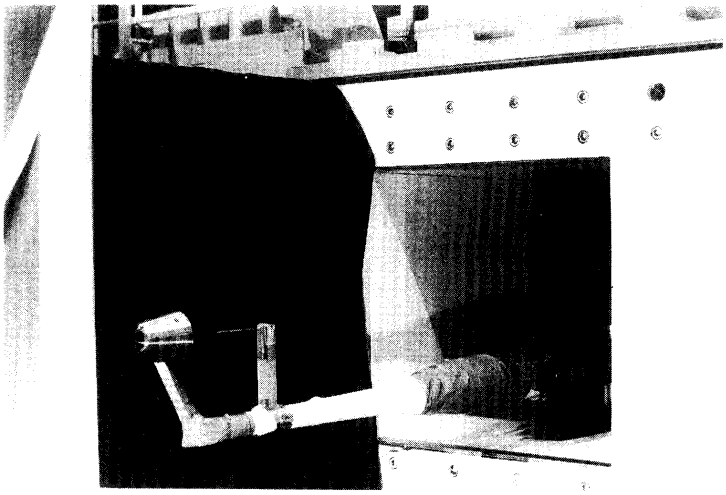

MODEL SETUP IN SUPERSONIC WIND TUNNEL

Fig. 4. Model Setups in Transonic and Supersonic Wind Tunnels.

surface by the strut which is fixed on the head of the sting mount as shown in Fig. 5. The distance between the center line of the model and that of the sting is set to be about twice the model base diameter. The axis of the capsule model coincides with the center line of the test section. The angle of attack is fixed as 0-deg. The static pressure and the Pitot pressure are measured by the static and Pitot pressure probes set on the traversing mount, respectively. The traversing mount is fixed on the sting mount and the traverse is made in the freestream direction. When the model is fixed in the flow by such kind of the support system, the wake flow field may be significantly disturbed by the model support, the traversing probes and their mount. The flow visualizations by the schlieren method are expected to clarify not only the structure of the wake flow field but also the influences of the disturbance produced by the model support system on the wake flow field.

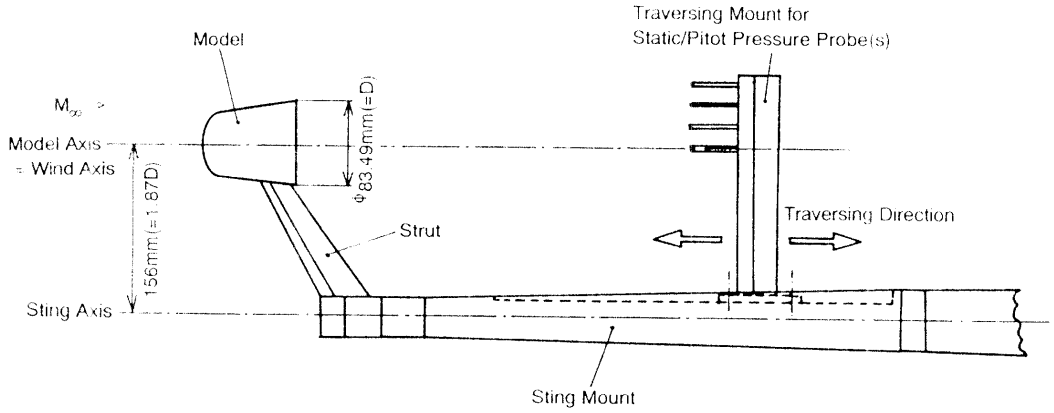

Fig. 5. Setup of Model and Traversing Probes in Wind Tunnel.

Figure 6 shows the measuring points at the traverse in the present experiments. The Pitot pressure is measured at four y-location, that is, at y=0, 0.25D, 0.5D and 0.75D, simultaneously by using the traversing rake of the four Pitot probes, while the static pressure is measured only on the capsule body axis, that is, at y=0, as shown in Fig. 7. The traverse in the freestream direction (x-direction) is made from 1.68D to 5.27D (measured from the capsule bottom). During the wind tunnel operation, the x-location is fixed and the measurement at a different x-location is made at another run of the wind tunnel.

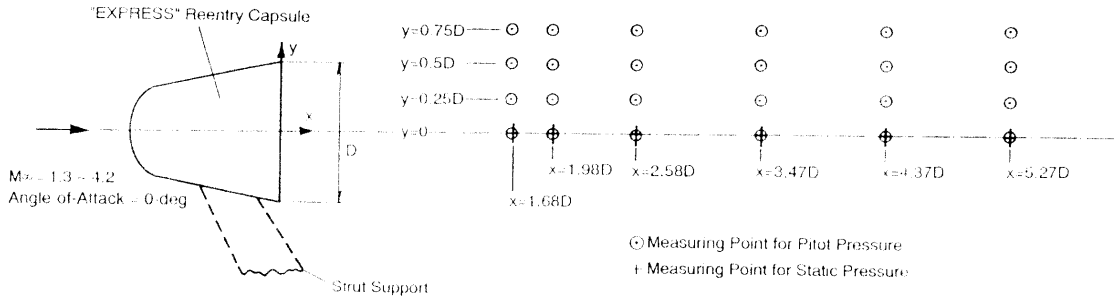

Fig. 6. Measuring Points for Pitot Pressure and Static Pressure in Wake Region.

In the measurement of the Pitot pressure and the static pressure, the configuration and the attitude of the probes have significant influences on the accuracy of the measured data. Figure 8 shows the configuration of the traversing rake of the four Pitot probes, each of which is made of the stainless tube. As for the Pitot pressure, the accuracy of the measured data may be spoiled by the following causes as:

(1) the deviation of the probe direction from the local flow direction.
(2) the disturbance made by the traversing mount of the probes.
(3) the disturbance made by the other Pitot probes in the rake.
(4) the disturbance made by the model support.

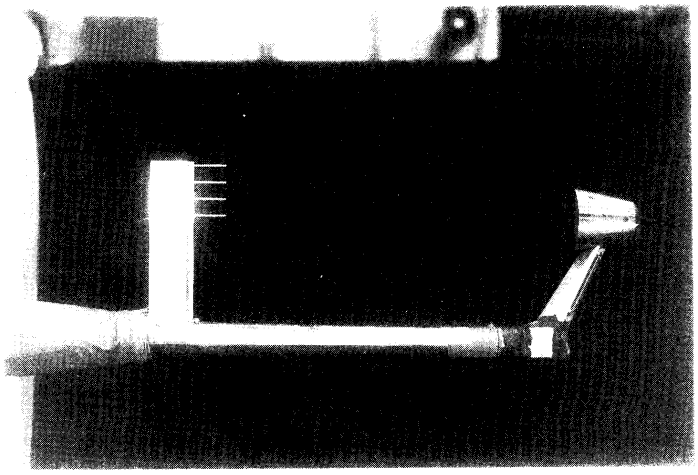

RAKE OF FOUR PITOT PRESSURE PROBES

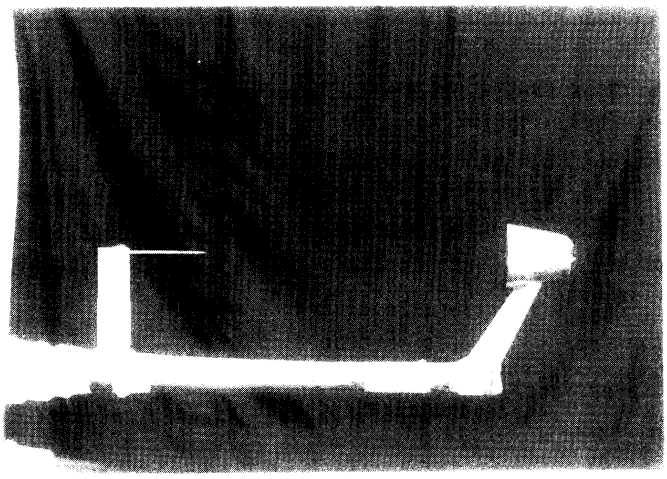

STATIC PRESSURE PROBE

Fig. 7 Pitot Pressure Probes and Static Pressure Probe

The effect of the item (1) is expected to be small in the present study, since the traversing area is located in the downstream from the recirculating region and the flow is almost parallel to the freestream and the Pitot pressure is not so sensitive to the deviation of the probe direction from the flow direction [5]. The effects of the items (2) and (3) are also expected to be small, since the flow is expected to be supersonic at almost all the measuring points and the disturbances made by the probes and traversing mount are essentially propagated to the downstream. As for the item (4), however, the effects of the model support are not necessarily negligibly small and they should be clarified by the schlieren pictures.

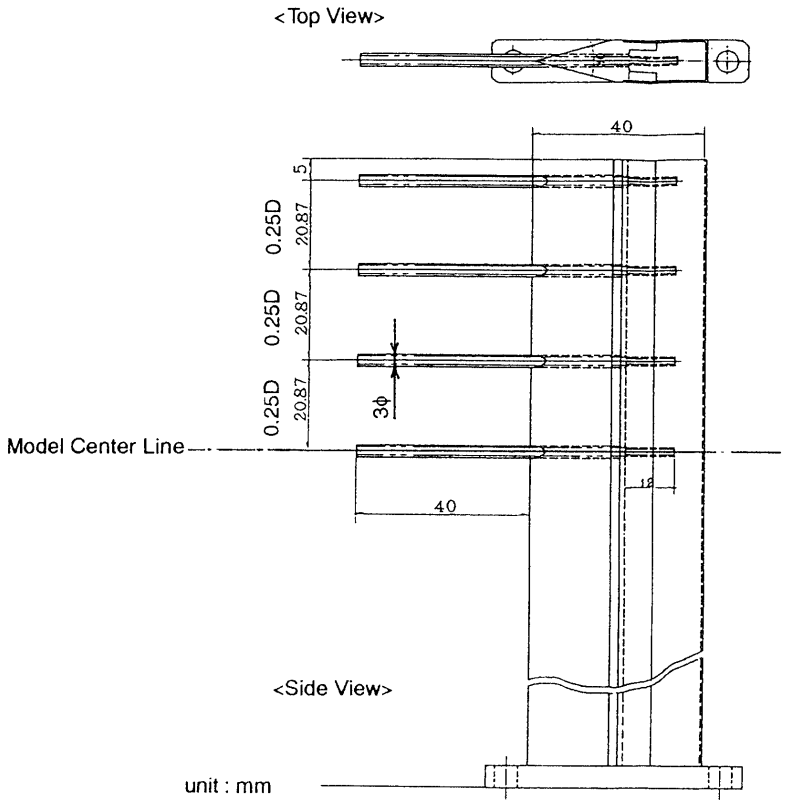

Fig. 8. Configuration of Traversing Rake of Four Pitot Probes.

The accuracy of the static pressure measurement strongly depends on the probe configuration and its attitude in the flow. Figure 9 shows the configuration of the static pressure probe used in the present experiments. The probe consists of the conical nose cap and cylindrical tube with four pressure ports. For the acquisition of the undisturbed data for the static pressure, the following requirement for the probe should be satisfied [*5*]:

(1) To make the conical cap as sharp as possible,
(2) To put the pressure port as far as possible from the shoulder of the conical part,
(3) To put the probe in parallel to the local flow direction.

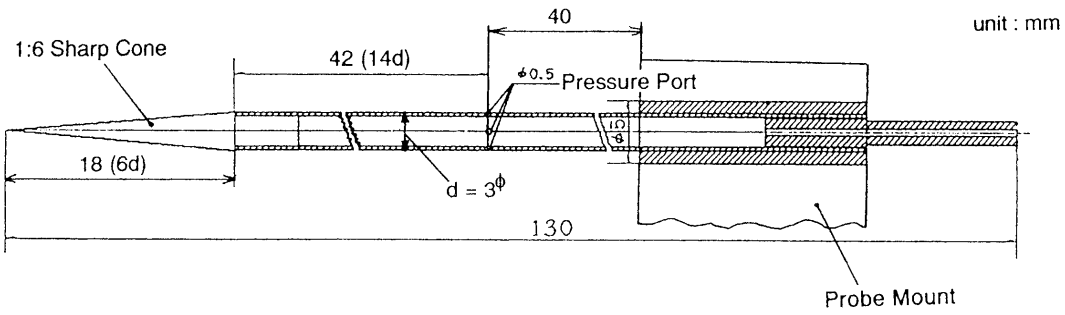

Fig. 9. Configuration of Static Pressure Probe.

As for the item (2), there is an experimental evidence as shown in Fig. 10 (from ref. 6). It is clear that the distance between the conical junction and the pressure orifice should be at least ten-times of the probe diameter. In the present study, the static pressure probe has a nose cap of a very sharp cone and the sufficiently large distance between the junction and the pressure orifices. Then as for the items (1) and (2), the present probe has a favorable nature with respect to the accuracy of the measurement data. In the present study, the static pressure is measured only on the model center line on which the flow is essentially parallel to the freestream direction, since the accuracy of the static pressure measured by such kind of probe is known to be very sensitive to the deviation of the probe direction from the local flow direction [*5*, *6*].

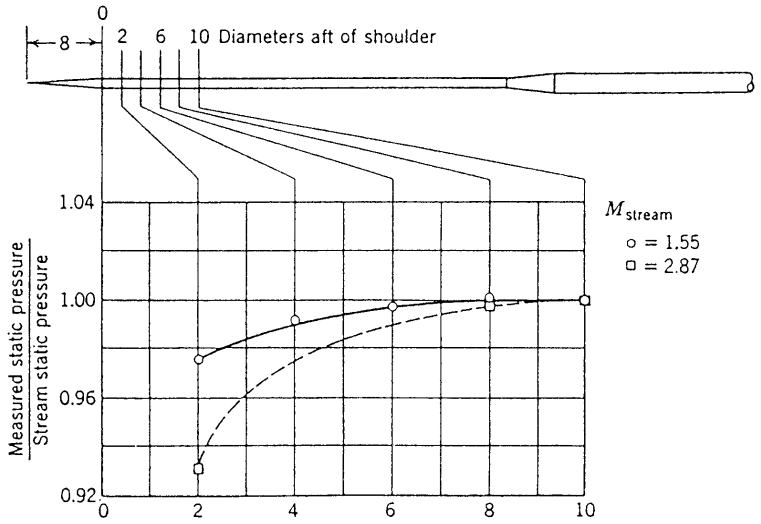

Fig. 10. Effect of Distance between Pressure Orifice and Probe Shoulder on Accuracy of Static Pressure Measurement (from Ref. 6).

Both the Pitot pressure and the static pressure are transferred to the pressure transducers which are located outside the test section via flexible tubes. The experimental data measured at the rate of 10-Hz are averaged in time over 10-sec. Their temporal variations are not discussed in the present study, since in the present experiments the unsteadiness of the wake flow field is not significant.

Method of Data Processing

In the present study, the spatial distributions of the Pitot pressure and the static pressure are measured by traversing the Pitot and static pressure probes, respectively. The Pitot pressure is normalized by the freestream Pitot pressure or the stagnation pressure. Since the uniform flow is always supersonic in the present experiments, the Pitot pressure is not equal to the stagnation pressure of the uniform flow due to the normal shock in front of the probe. The freestream Pitot pressure is obtained by the Rayleigh's Pitot formula [5]:

$$\frac{p_0}{p_{Pitot\,\infty}} = \left(\frac{2\gamma}{g+1} M_\infty^2 - \frac{\gamma-1}{g+1}\right)^{\frac{1}{\gamma-1}} \left(\frac{1+\frac{\gamma-1}{2}M_\infty^2}{\frac{\gamma+1}{2}M_\infty^2}\right)^{\frac{\gamma}{\gamma-1}}, \tag{1}$$

where the p_0 is the settling chamber pressure.

In the present experiments, the static pressure is measured only on the center line of the body. The local Mach number, the local total pressure and the local dynamic pressure are computed on the center line. When the wake flow field is not disturbed strongly by the model support system, the flow direction on the center line is expected to coincide with the uniform flow direction, that is, the probe direction. Then the local Mach number M in the subsonic region is computed by assuming that the flow is isentropic and that the total pressure equals to the Pitot pressure:

$$\frac{p_{pitot}}{p} = \left(1 + \frac{\gamma - 1}{2} M\right)^{\frac{\gamma}{\gamma-1}}, \tag{2}$$

where p is the local static pressure. In the supersonic flow, the Pitot pressure is different from the total pressure because of the shock wave generated in front of the Pitot probe and the Rayleigh's Pitot formula should be used for computation of the local Mach number as:

$$\frac{p}{p_{Pitot}} = \frac{\left(\frac{2\gamma}{\gamma+1} M^2 - \frac{\gamma-1}{\gamma+1}\right)^{\frac{1}{\gamma-1}}}{\left(\frac{\gamma+1}{2} M^2\right)^{\frac{\gamma}{\gamma-1}}}. \tag{3}$$

The local total pressure is calculated by the relation:

$$p_0 = \left(1 + \frac{\gamma-1}{2} M^2\right)^{\frac{\gamma}{\gamma-1}} p. \tag{4}$$

The local dynamic pressure is computed by the relation:

$$q = \frac{1}{2} \gamma M^2 p \,. \tag{5}$$

3. NUMERICAL ANALYSIS

To deepen our understanding on the structure of the wake flow field, the numerical simulations of the flow field around the capsule body including the base flow region are carried out at Mach numbers 4.2 and 20.6 by solving the laminar axi-symmetric Navier-Stokes equations. The Rational Runge-Kutta (RRK) scheme [7] and Yee's symmetric TVD scheme [8] are used for the time integration scheme and the finite differencings of the convective terms of the equations, respectively. The grid topology for the present study is O-type around the body and the number of the grid points is 61 in the longitudinal direction and 101 in the radial direction. The case at Mach number 4.2 is made to duplicate the supersonic wind tunnel experiment and the case at Mach number 20.6 corresponds to the practical reentry flight condition at altitude 50-km. In the present calculations, the flow is assumed to be laminar everywhere. This assumption is appropriate with respect to the boundary layer over the body surface. In fact, a series of the experimental flow visualizations made for the present configuration by the China-clay method demonstrate that the boundary layer is laminar over the forebody of the capsule at Mach numbers higher than 3 in the present range of the freestream Reynolds number. As for the wake flow region, however, the transition may occur in the wake core behind the wake neck as explained in Fig. 1.

4. RESULTS AND DISCUSSIONS

Effects of Model Support and Flow Unsteadiness

Figure 11 shows the schlieren pictures at Mach numbers 1.3, 2.0 and 4.2. The wake structure which consists of the shear-layer, recirculating region, wake-neck, trailing shock, wake-core and so on as explained in Fig. 1 is clearly shown in these pictures. The influences of the strut-sting model support system on the wake flow field are observed at each Mach number. Such influences become weaker at higher Mach number, since the interaction between the bow shock wave over the model and the shock wave generated by the model support occurs far downstream when the Mach number is high. Due to the disturbances generated by the model support, the wake flow field is distorted to be slightly unsymmetric with respect to the model center line at each Mach number. In the following discussions, we assume the mirror image of the upper part of the picture by the symmetric inversion with respect to the model center line, since the influences of the model support on the wake flow field are expected to be negligibly small in the upper part of the picture.

The unsteadiness in the wake flow field is not significant both in the schlieren picture and in the temporal variations of the Pitot pressure and the static pressure.

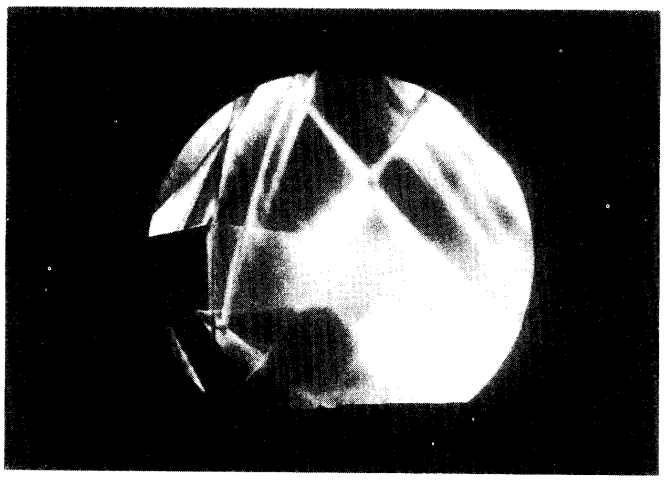

M = 1.3

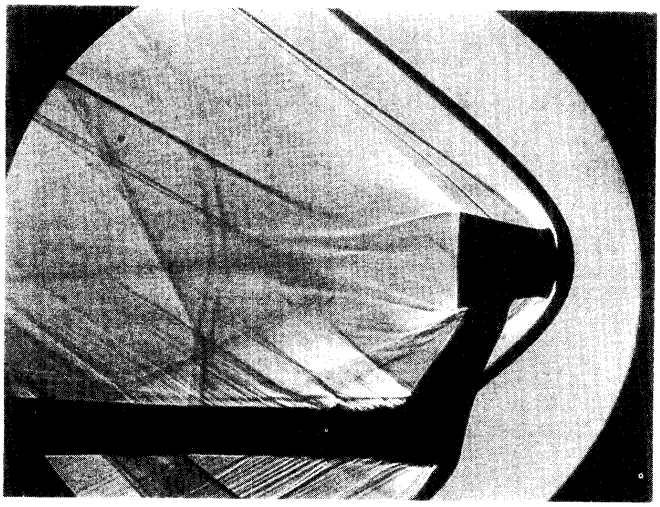

M = 2.0

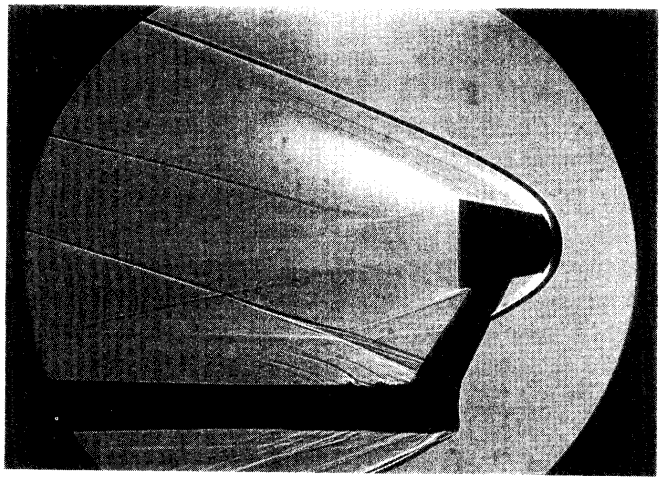

M = 4.2

Fig. 11 Schlieren Photographs of Wake Flow behind Capsule Model.

Effects of Freestream Reynolds Number

Figure 12 shows the effects of the freestream Reynolds number on the wake flow field in the Reynolds number sweep test. The Mach number is fixed as 3.0. We evaluate the properties of the wake flow field by the diameter of the wake core at the wake neck, the distance from the model base to the wake neck and the Pitot pressure measured at x/D=3.47 on the center line. The former two items are classified into the geometric parameters which define the configuration of the wake structure and are determined by analyzing the schlieren picture. The results show that in the present experiments the effects of the freestream Reynolds number on the wake flow field are negligibly small in comparison with those of the freestream Mach number.

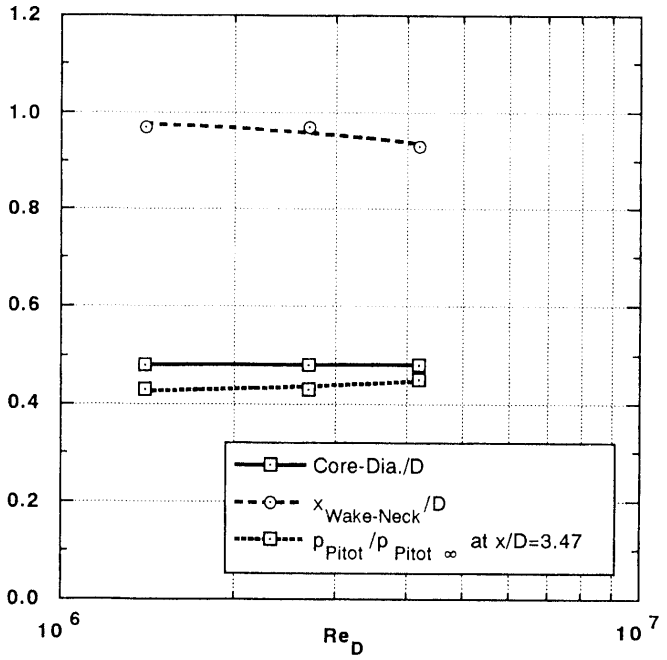

Fig. 12. Effects of Reynolds Number on Wake Flow Field.

Comparisons between Schlieren Picture and Pitot Pressure Distribution

Figures 13, 14 and 15 show the comparisons between the Pitot pressure distributions and the schlieren photographs at Mach numbers 1.3, 2.0 and 4.2, respectively. The shear-layer which develops from the base corner and the boundary of the wake core are clearly observed in the schlieren picture. The wake neck is identified as the intersecting point of the shear-layer and the boundary line of the wake core. The trailing shock wave issued from the wake neck regime is observed at Mach numbers 2.0 and 4.2. At Mach number 1.3, however, the trailing shock is not observed. The schlieren picture shows that all the measuring points for the Pitot pressure and the static pressure are located in the downstream region of the wake neck (namely outside the recirculating region) at Mach numbers 2.0 and 4.2, while at Mach number 1.3 the most forward measuring points (x=1.68D) may be located in the reverse flow region. These schlieren pictures clarify the fact that the wake neck goes upstream and diameter of the wake core decreases when the Mach number increases.

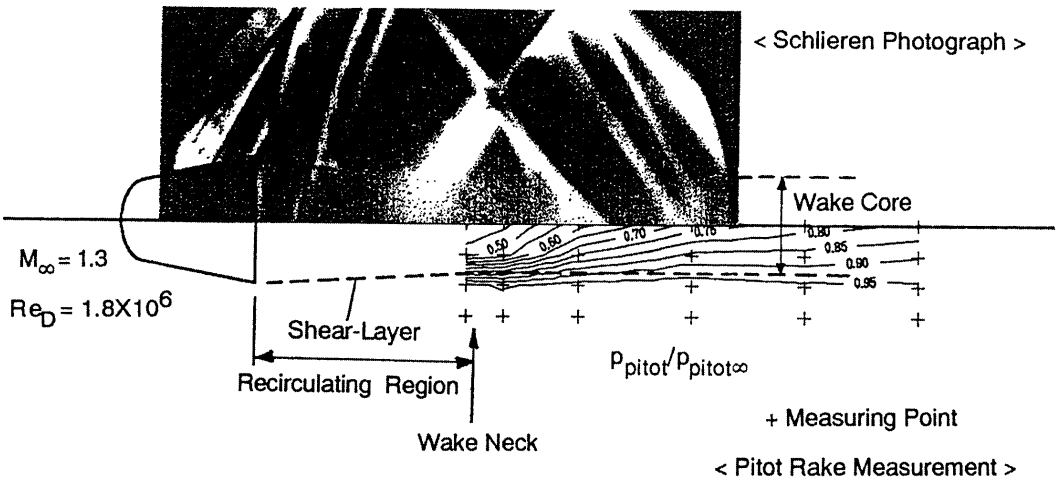

Fig. 13. Schlieren Photograph and Pitot Pressure Distribution in Wake at Mach Number 1.3.

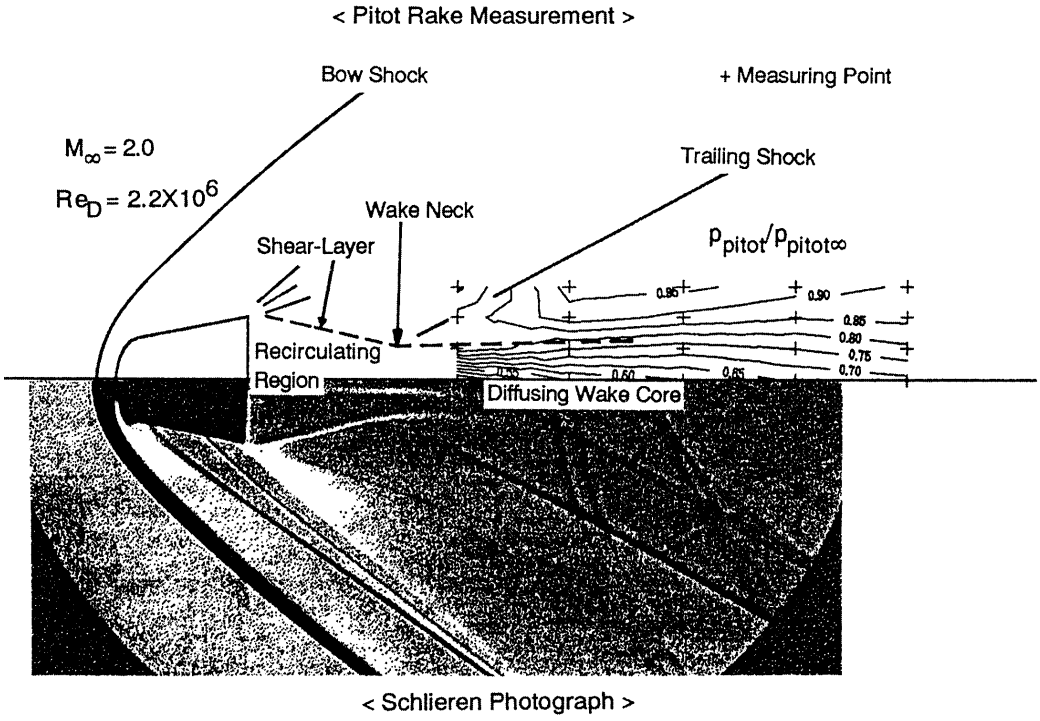

Fig. 14. Schlieren Photograph and Pitot Pressure Distribution in Wake at Mach Number 2.0.

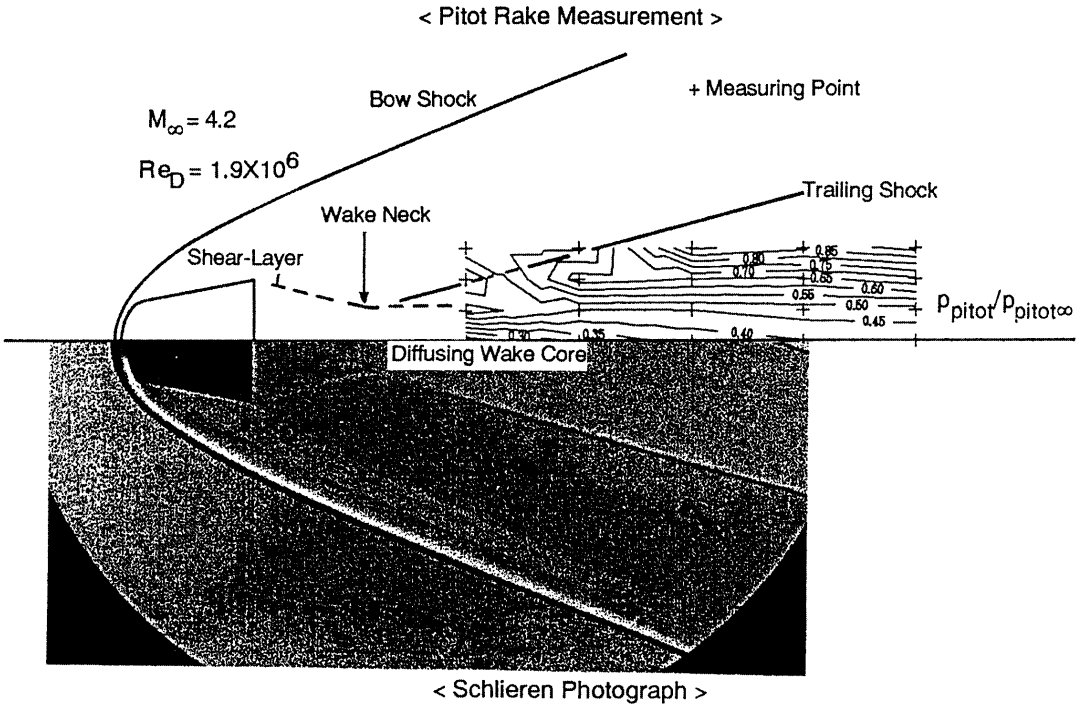

Fig. 15. Schlieren Photograph and Pitot Pressure Distribution in Wake at Mach Number 4.2.

In the downstream region of the wake neck, the Pitot pressure increases both in the freestream direction (x-direction) and in the radial direction away form the center line of the wake (y-direction). The contour lines of the Pitot pressure normalized by the freestream value are almost parallel to the freestream direction and this fact indicates that there is a strong gradient of the Pitot pressure in the radial direction (y-direction). At Mach number 1.3, the contour lines of the Pitot pressure are observed only inside the wake core and the line of 95% recovery almost coincides with the boundary of the wake core. At Mach numbers 2.0 and 4.2, however, the contour lines of the Pitot pressure are also observed outside the wake core and the contour lines are distorted across the trailing shock wave.

From the above discussions, it is concluded that the structure of the wake flow field behind a supersonic body of capsule type is classified into two categories, that is, the subsonic wake neck type and the supersonic wake neck type. In the former type, the flow is subsonic at the wake neck and the trailing shock wave is not formed. In the latter type, the flow is supersonic at the wake neck and the trailing shock is formed. The wake flow of the former type is accompanied by much larger recirculating region behind the bottom of the body and the wake core having a larger diameter than the wake flow of the latter type. When the freestream Mach number increases, the structure of the wake flow field is transformed from the subsonic wake neck type to the supersonic wake neck type. In the present experiments, the case at Mach number 1.3 belongs to the former type and the cases at Mach numbers 2.0 and 4.2 belong to the latter type.

Recovery of Dynamic Pressure on Center Line

Figure 16 shows the distribution of the local Mach number on the center line at Mach numbers 1.3, 2.0 and 4.2. The local Mach number increases both with the increase in the distance from the model base and with the freestream Mach number. At each Mach number, there seems to be the far downstream limit value to which the local Mach number asymptotically increases when the flow goes to the infinitely far downstream. The far downstream limit values for the local Mach number are estimated to be about 1.3, 1.8 and 2.1 for freestream Mach numbers 1.3, 2.0 and 4.2, respectively.

At Mach number 1.3, the local Mach number is almost zero at the distance around 2D from the capsule bottom. The rear stagnation point, at which the local flow velocity vanishes in the wake, is expected to be located in this region.

The local Mach number at the wake neck plays an important role in determining the structure of the wake flow field, since the trailing shock wave is formed when the flow is supersonic in the wake neck region. At Mach number 1.3, the flow is subsonic at the distance less than 4D from the capsule bottom and the flow at the wake neck is also subsonic. On the other hand, at Mach numbers 2.0 and 4.2, the flow is supersonic even at the most forward measuring point (x=1.68D) and the flow at the wake neck is also supersonic. It can be judged also by the presence of the shock wave in front of the Pitot pressure probe whether the flow is supersonic or subsonic at the measuring point. Figure 17 shows the shock waves in front of the Pitot pressure probe at Mach number 2.

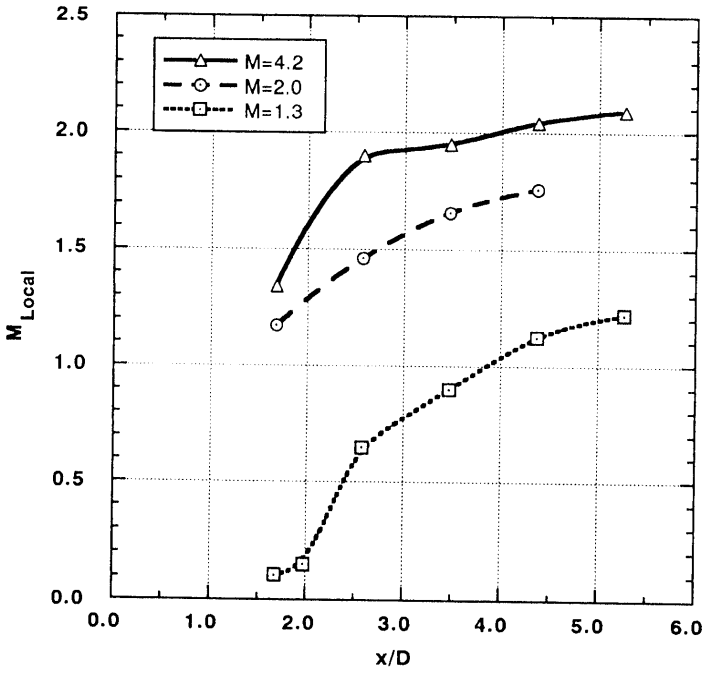

Fig. 16. Variation of Local Mach Number on the Center Line of Wake.

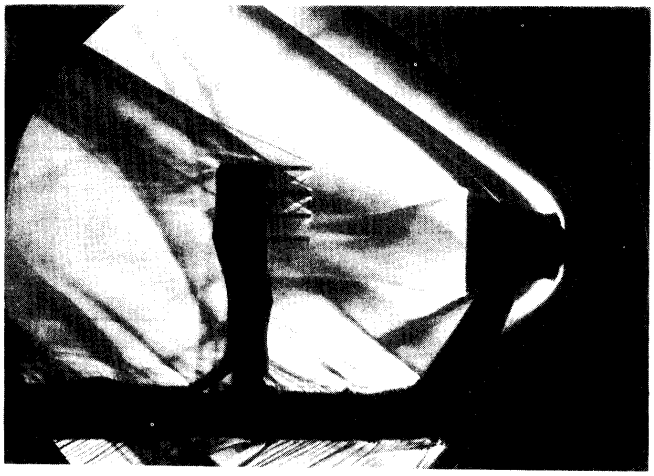

X = 1.68 D

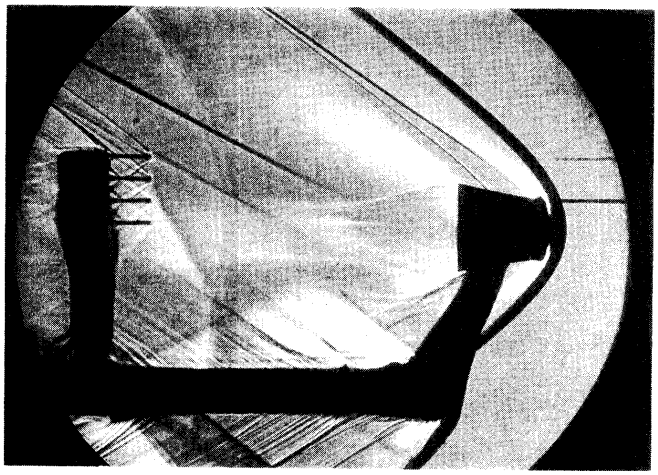

X = 2.58 D

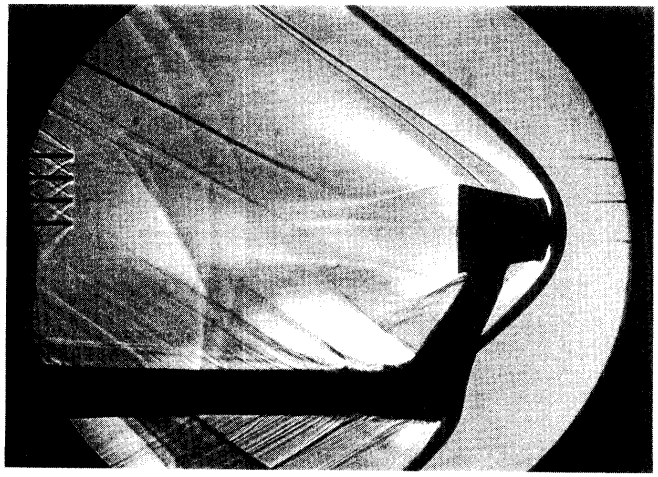

X = 3.47 D

Fig. 17. Schlieren Photographs of Shock Waves in front of Pitot Pressure Probes.

Figures 18, 19 and 20 show the variations of the recovery ratio, which is defined as the ratio of the local value to the freestream value, with the distance from the base for the local Mach number, the total pressure and the dynamic pressure, respectively. When the flow goes infinitely far downstream, the recovery ratio does not necessary become the unity. At Mach number 4.2, the local Mach number and the total pressure at the infinitely far downstream are expected to be only 50% and 10% of their freestream values, respectively.

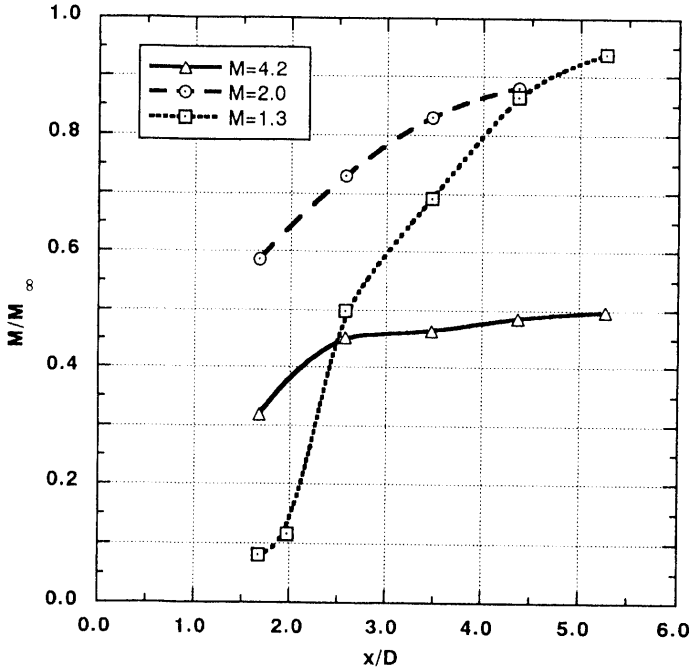

Fig. 18. Recovery Ratio of Total Pressure on the Center Line of Wake.

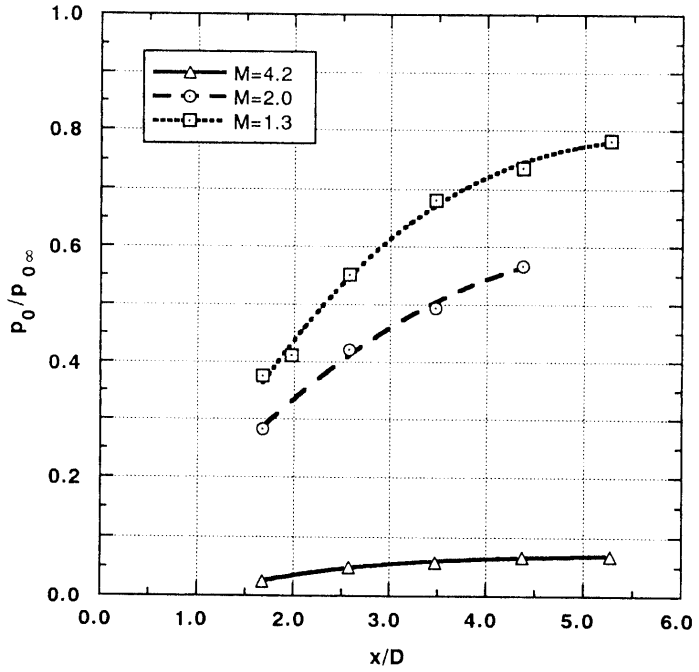

Fig. 19. Recovery Ratio of Total Pressure on the Center Line of Wake.

From a viewpoint of the parachute deployment, the distribution of the dynamic pressure is the most important information in the present study. Figure 20 shows that the dynamic pressures at the infinitely far downstream are estimated as about 80%, 65% and 40% of the freestream value at Mach numbers 1.3, 2.0 and 4.2, respectively. At Mach number 1.3, the structure of the wake flow field is classified into the subsonic wake neck type and the recirculating region behind the capsule bottom extends over twice of the base diameter. However, as for the dynamic pressure at the distance 5D from the capsule bottom, where the parachute will be deployed, the highest recovery ratio is obtained at Mach number 1.3, since at Mach number 1.3 the dynamic pressure increases more rapidly in the downstream direction behind the recirculating region than at the other Mach numbers. In the far downstream region, a higher recovery ratio is obtained for the dynamic pressure at lower freestream Mach number. When the Mach number decreases, however, the recovery of the dynamic pressure may be significantly delayed, since the structure of the wake is changed from the supersonic wake neck type to the subsonic wake neck type and the recirculating region may extend far downstream.

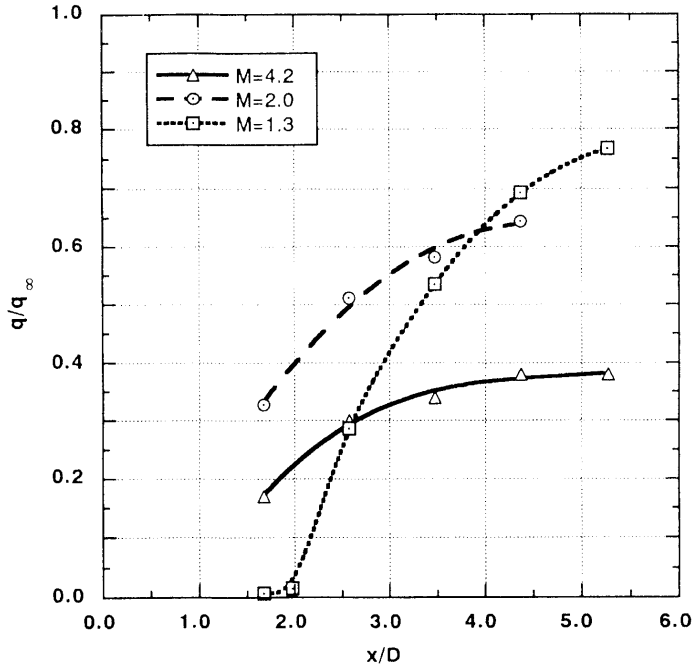

Fig. 20. Recovery of Dynamic Pressure on the Center Line of Wake.

Effects of Mach Number on Wake Flow Properties

Figure 21 shows the variations of the recovery ratios of the local Mach number, the dynamic pressure and the total pressure with the Mach number measured at x=3.47D. When the freestream Mach number is higher than 2, the recovery ratios decrease with the increase in the Mach number and seem to reach asymptotically their hypersonic limit values which are independent of the Mach number. The hypersonic limit values for the recovery ratios of the local Mach number, the dynamic pressure and the total pressure are estimated to be about 40%, 30% and 5%, respectively. On the other hand, when the Mach number is less than 2.0, the recovery ratios of the local Mach number and the dynamic pressure decrease with the decrease in the Mach number because of the presence of the recirculating region which extends far downstream.

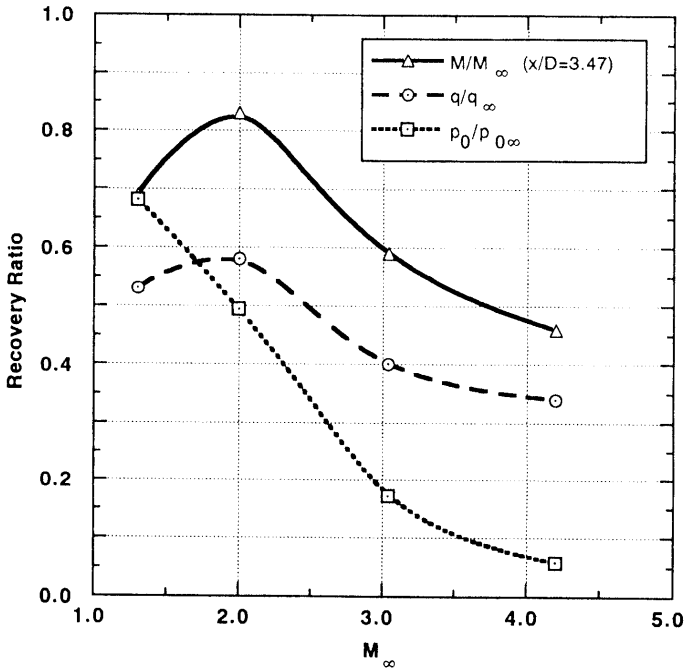

Fig. 21. Variation of Recovery Ratio of Local Mach Number, Total Pressure and Dynamic Pressure with Freestream Mach Number at x = 3.47D.

Figure 22 shows the variations of the diameter of the wake core and the distance between the wake neck and the capsule bottom with the freestream Mach number. These values are very important for the definition of the configuration of the wake behind the capsule body. When the Mach number increases, these values decrease and reach asymptotically their hypersonic limit values. This fact indicates that the wake core shrinks and the wake neck moves upstream with the increase in the freestream Mach number. At Mach number less than 2.0, the wake neck moves downstream rapidly with the decrease in the Mach number, since the recirculating region behind the capsule bottom extends downstream rapidly with the decrease in the Mach number due to the change in the structure of the wake flow field from the supersonic wake neck type to the subsonic wake neck type. When the Mach number is higher than 2.0, the diameter of the wake core is almost constant at about 50% of the base diameter.

The numerical results by the Navier-Stokes analysis are also plotted in Fig. 22. At Mach number 4.2, the numerical results show a good agreement with the experimental results. The numerical results for the wake core diameter and the distance between the wake neck and the capsule base at Mach number 20.6 are 0.55D and 0.65D, respectively. Considering the experimental results at Mach

number 4.2, the present Navier-Stokes analysis is expected to provide a good estimation on the configuration of the wake behind a capsule body.

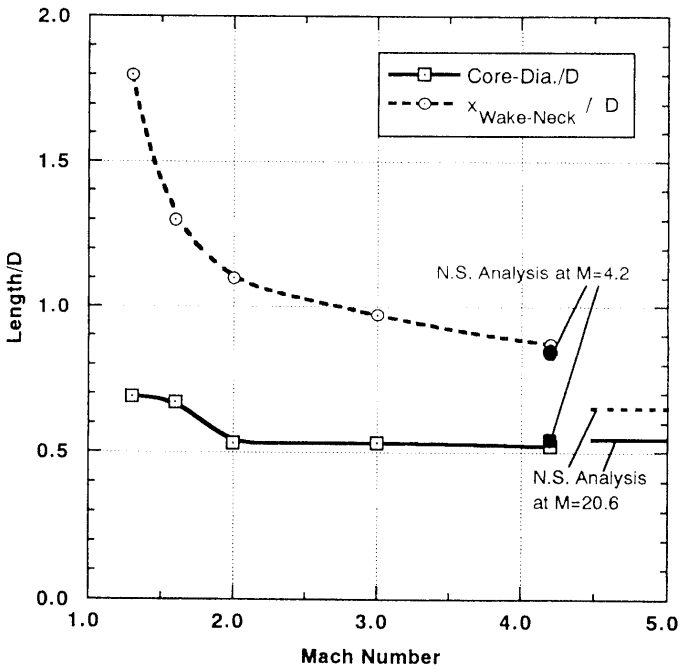

Fig. 22. Effects of Mach Number on Diameter of Wake Core and Location of Wake Neck.

Comparisons with Numerical Analysis

Figure 23 shows the comparison of the distribution of the Pitot pressure between the experimental results and the numerical results at Mach number 4.2. As for the locations of the bow shock wave, the trailing shock wave, the shear-layer, the wake neck and the wake core, they are in good agreement. As for the Pitot pressure in the wake region, however, the numerical results are

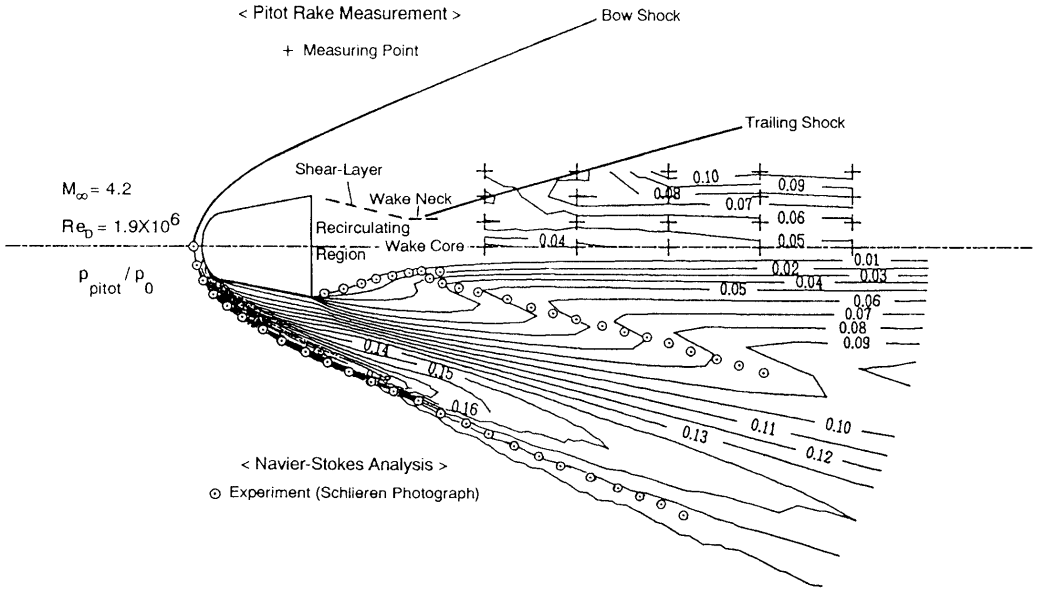

Fig. 23. Comparison between Numerical Result and Experimental Result on Pitot Pressure Distribution at Mach Number 4.2.

much less than the experimental results especially in the vicinity of the center line of the wake. In the Navier-Stokes analysis, the flow is assumed to be laminar in the whole flow field including the wake region. If the turbulent transition occurs behind the wake neck as shown in Fig. 1, the recovery of the flow velocity in the wake core may be significantly enhanced by the turbulent transport in the normal direction (y-direction). Then the spatial distributions of the dynamic pressure and the Pitot pressure in the wake region may be significantly affected by the turbulent transition behind the wake neck.

Figure 24 shows the distribution of the static pressure and the streamlines computed at Mach number 4.2. In the wake core, the pressure gradient exists in the freestream direction (x-direction) and the pressure is almost constant in the normal direction (y-direction). It is clear that the place at the minimum pressure in the recirculating region corresponds to the focus of the recirculating streamlines. In the recirculating region, the static pressure is less than the freestream static pressure. In the wake core, the static pressure is almost equal to the freestream pressure behind the rear stagnation point which is located at x=1.8D. According to the empirical relation [*3*], the static pressure in the wake core recovers to the freestream value at the location:

$$x/D = M^2/9. \tag{6}$$

At the Mach number 4.2, the right hand side of eq. (6) is 1.96 and this value is very close to the distance between the rear stagnation point and the capsule bottom in the present Navier-Stokes analysis.

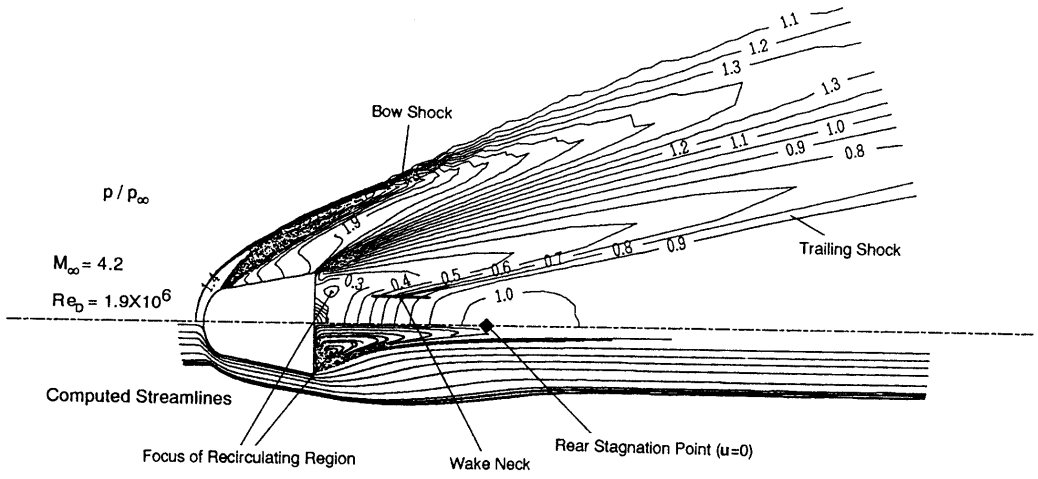

Fig. 24. Pressure Distribution and Streamlines in Navier-Stokes Analysis at Mach Number 4.2.

5. CONCLUDING REMARKS

A series of the experimental investigations on the wake flow field behind the "EXPRESS" capsule at supersonic speeds have been carried out by using the transonic and supersonic wind tunnels. The major conclusions are as follows:

(1) The structure of the wake flow field behind the capsule is clarified in the schlieren photographs and the distributions of the Pitot pressure and the static pressure. The structure of the wake is classified into two types, that is, the subsonic wake neck type and the supersonic wake neck type. In the wake of the former type, the recirculating region extends far downstream. In the

wake flow of the latter type, the trailing shock wave is formed at the wake neck. In the present case, when the Mach number decreases from 2.0 to 1.3, the wake structure is changed from the supersonic wake neck type to the subsonic wake neck type.

(2) When the freestream Mach number increases, the diameter of the wake core shrinks and the wake neck moves upstream. When the Mach number becomes large, the structure of the wake flow field becomes independent of the Mach number and the diameter of the wake core is almost constant at 50% of the base diameter.

(3) The variation of the dynamic pressure in the wake core with the distance from the capsule bottom is obtained experimentally at Mach numbers from 1.3 to 4.2 by using the static pressure probe and the Pitot pressure probes. When the flow goes downstream behind the recirculating region, the dynamic pressure increases and asymptotically reaches the far downstream limit value, which is less than the freestream dynamic pressure.

(4) In the far downstream region, a higher recovery ratio is obtained for the dynamic pressure at lower freestream Mach number. When the Mach number decreases, however, the recovery of the dynamic pressure in the wake core may be significantly delayed, since the structure of the wake is changed from the supersonic wake neck type to the subsonic wake neck type and the recirculating region extends far downstream.

(5) As for the structure of the wake flow field, the laminar Navier-Stokes analysis provides a qualitatively good estimation in comparison with the experimental results. As for the recovery of the velocity in the wake core, however, the turbulent transition should be considered, since it may be enhanced significantly by the turbulent transport in the normal direction to the center line of the wake.

ACKNOWLEDGMENT

The authors would like to present special thanks to Mr. Hongoh, technical staff of the ISAS wind tunnel test facility, for his helpful support in the operation of the transonic and supersonic wind tunnels.

REFERENCES

[1] ZIMBERLIN, J., YAMAZAKI, A. AND HINADA, M.: EXPRESS – a Reusable Technology Carrier, Proc. 18th Int. symp. on Space Tech. Sci. (1992).

[2] HIRAKI, K.: Private Communication.

[3] LYKOUDIS, P.S.: A Review of Hypersonic Wake Studies, AIAA J., Vol. **4**, No. 4, pp. 577-590 (1966).

[4] STRAWA, A.W., PARK, C., DAVY, W.C., BABIKIAN, D.S. AND PRABHU, D.K.: Proposed Radiometric Measurement of the Wake of a Blunt Aerobrake, J. Spacecraft and Rockets, Vol. **29**, No. 6, pp. 765-772 (1992).

[5] LIEPMANN, H.W. AND ROSHKO, A.: Elements of Gasdynamics, John Wiley & Sons, (1960).

[6] POPE, A. AND GOIN, K.L.: High-Speed Wind Tunnel Testing, John Wiley & Sons, (1965).

[7] SATOFUKA, N.: Numerical Solution of the Euler and Navier-Stokes Equations on Parallel Computers, Proc. Int. symp on Computational Fluid Dynamics, Nagoya 1989, pp. 28-34 (1989).

[8] YEE, H.C.: A Class of High-Resolution Expicit and Implicit Shock-Capturing Methods, NASA TM 101088 (1989).